Immune Netw. 2024 Apr;24(2):e3
https://doi.org/10.4110/in.2024.24.e3
pISSN 1598-2629·eISSN 2092-6685

IMMUNE NETWORK

Original Article

Cigarette Smoke Extract-Treated Mouse Airway Epithelial Cells-Derived Exosomal LncRNA MEG3 Promotes M1 Macrophage Polarization and Pyroptosis in Chronic Obstructive Pulmonary Disease by Upregulating TREM-1 via m^{6}A Methylation

Lijing Wang [1], **Qiao Yu** [1], **Jian Xiao** [1], **Qiong Chen** [1], **Min Fang** [2], **Hongjun Zhao** [3,*]

[1]Department of Geriatrics, National Clinical Research Center for Geriatric Disorders, Xiangya Hospital, Central South University, Changsha 410008, China
[2]Hunan Provincial Key Laboratory of the Research and Development of Novel Pharmaceutical Preparations, the "Double-First Class" Application Characteristic Discipline of Hunan Province (Pharmaceutical Science), Changsha Medical University, Changsha 410219, China
[3]Department of Rheumatology and Immunology, Xiangya Hospital, Central South University, Changsha 410008, China

Received: Oct 18, 2023
Revised: Dec 13, 2023
Accepted: Jan 2, 2024
Published online: Jan 19, 2024

***Correspondence to**
Hongjun Zhao
Department of Rheumatology and Immunology, Xiangya Hospital, Central South University, No. 87 Xiangya Road, Changsha 410008, China.
Email: zhaohj022@sohu.com

ORCID iDs
Lijing Wang
https://orcid.org/0000-0003-1983-7348
Qiao Yu
https://orcid.org/0000-0001-5893-9086
Jian Xiao
https://orcid.org/0000-0003-2761-1779
Qiong Chen
https://orcid.org/0000-0002-2534-8834
Min Fang
https://orcid.org/0009-0008-7452-5500
Hongjun Zhao
https://orcid.org/0009-0002-0866-3872

Conflict of Interest
The authors declare no potential conflicts of interest.

ABSTRACT

Cigarette smoke extract (CSE)-treated mouse airway epithelial cells (MAECs)-derived exosomes accelerate the progression of chronic obstructive pulmonary disease (COPD) by upregulating triggering receptor expressed on myeloid cells 1 (TREM-1); however, the specific mechanism remains unclear. We aimed to explore the potential mechanisms of CSE-treated MAECs-derived exosomes on M1 macrophage polarization and pyroptosis in COPD. *In vitro*, exosomes were extracted from CSE-treated MAECs, followed by co-culture with macrophages. *In vivo*, mice exposed to cigarette smoke (CS) to induce COPD, followed by injection or/and intranasal instillation with oe-TREM-1 lentivirus. Lung function and pathological changes were evaluated. CD68$^+$ cell number and the levels of iNOS, TNF-α, IL-1β (M1 macrophage marker), and pyroptosis-related proteins (NOD-like receptor family pyrin domain containing 3, apoptosis-associated speck-like protein containing a caspase-1 recruitment domain, caspase-1, cleaved-caspase-1, gasdermin D [GSDMD], and GSDMD-N) were examined. The expression of maternally expressed gene 3 (MEG3), spleen focus forming virus proviral integration oncogene (SPI1), methyltransferase 3 (METTL3), and TREM-1 was detected and the binding relationships among them were verified. MEG3 increased N6-methyladenosine methylation of TREM-1 by recruiting SPI1 to activate METTL3. Overexpression of TREM-1 or METTL3 negated the alleviative effects of MEG3 inhibition on M1 polarization and pyroptosis. In mice exposed to CS, EXO^{-CSE} further aggravated lung injury, M1 polarization, and pyroptosis, which were reversed by MEG3 inhibition. TREM-1 overexpression negated the palliative effects of MEG3 inhibition on COPD mouse lung injury. Collectively, CSE-treated MAECs-derived exosomal

IMMUNE NETWORK

Abbreviations

ASC, apoptosis-associated speck-like protein containing a caspase-1 recruitment domain; BAL, bronchoalveolar lavage; BALF, bronchoalveolar lavage fluid; BCA, bicinchoninic acid; ChIP, chromatin immunoprecipitation; COPD, chronic obstructive pulmonary disease; CS, cigarette smoke; CSE, cigarette smoke extract; FCM, flow cytometry; FEV0.4/FVC, forced expiratory volume in 0.4 s/forced vital capacity; GSDMD, gasdermin D; lncRNA, long non-coding RNA; MAEC, mouse airway epithelial cell; MAN, mean alveolar number; MEG3, maternally expressed gene 3; MeRIP, methylated RNA immunoprecipitation; METTL3, methyltransferase 3; MLI, mean linear intercept; m6A, N6-methyladenosine; NLRP3, NOD-like receptor family pyrin domain containing 3; PAR-CLIP, photoactivatable ribonucleoside-enhanced crosslinking and immunoprecipitation; PEF, peak expiratory flow; RIPA, radio-immunoprecipitation assay; RT-qPCR, reverse transcription quantitative PCR; SPI1, spleen focus forming virus proviral integration oncogene; TREM-1, Triggering receptor expressed on myeloid cells 1.

Author Contributions

Conceptualization: Wang L; Data curation: Wang L, Xiao J, Fang M, Zhao H; Formal analysis: Wang L, Yu Q; Funding acquisition: Wang L; Investigation: Wang L, Yu Q, Xiao J, Chen Q; Methodology: Wang L, Xiao J, Chen Q, Zhao H; Project administration: Wang L, Yu Q, Xiao J, Chen Q; Resources: Wang L, Yu Q; Software: Wang L, Yu Q; Supervision: Zhao H; Validation: Wang L; Visualization: Wang L; Writing - original draft: Wang L, Yu Q, Fang M; Writing - review & editing: Wang L, Yu Q, Fang M.

long non-coding RNA MEG3 may expedite M1 macrophage polarization and pyroptosis in COPD via the SPI1/METTL3/TREM-1 axis.

Keywords: LncRNA MEG3; TREM-1; SPI1; METTL3; M1 macrophage polarization

INTRODUCTION

Chronic obstructive pulmonary disease (COPD) is an inflammatory lung disease that causes restricted airflow and breathing problems, including emphysema, chronic bronchitis, or small airway obstruction (1). People with COPD often present with dyspnea, cough, and/or sputum production (2). Cigarette smoke (CS) exposure and air pollution are recognized as the most common environmental factors for COPD (3). At present, the treatment strategies of COPD are mainly for symptom improvement and exacerbation prevention, but there is no cure for COPD (4). With the aggravation of environmental pollution, aging population, and other problems, COPD prevention and treatment is becoming increasingly serious. Reportedly, CS extract (CSE) activate macrophages to release inflammatory mediators that speeds up COPD process (5,6). Inhibiting M1 macrophage polarization seems a feasible option for treating inflammatory diseases (7). Pyroptosis is widely present in respiratory diseases such as COPD, and excessive pyroptosis may be accompanied by airway inflammation, tissue damage, and poor prognosis (8). Therefore, the analysis of molecular mechanisms of COPD based on M1 macrophage polarization and pyroptosis may be a hopeful option for COPD treatment.

Macrophages are important immune cells in the body and play a key role in chronic inflammation in many lung diseases (9). Triggering receptor expressed on myeloid cells-1 (TREM-1), a member of the immunoglobulin superfamily, is largely enriched on the surface of myeloid cells including macrophages, monocytes, and neutrophils (10). A prior study illustrated that TREM-1 stimulated lung injury and inflammation in COPD mouse by mediating macrophage pyroptosis (11). Wang et al pointed out CSE-treated mouse airway epithelial cells (MAECs)-derived exosomes promoted M1 macrophage polarization by upregulating TREM-1 expression, thereby aggravating COPD progression (12). Nevertheless, which molecules in exosomes mediate the expression of TREM-1 needs further explorations.

Exosomes are cell-derived monolayer organelles with diameters of 30 to 200 nm, which have the same topological structure as cells and are rich in proteins, nucleic acids, glycoconjugates, and lipids (13). The implementation of exosomes in COPD development is gaining wide attention from many researchers. For example, human adipose-derived stem cells-derived exosomes could relieve CS-induced lung inflammatory response and injury by repressing alveolar macrophage pyroptosis (14). Endothelial progenitor cell-exosomal miR-26a-5p was reported to improve airway remodeling in COPD by repressing ferroptosis of bronchial epithelial cells (15). Notably, the mechanism of CS-stimulated exosome release in COPD mainly focuses on miRNAs (16), while other aspects are rarely reported.

Long non-coding RNA (lncRNA), a cluster of RNA transcripts with more than 200 nucleotides in length, has been documented to play an important role in various biological functions and be linked to many diseases including COPD (17). A preceding study revealed lncRNA maternally expressed gene 3 (MEG3) overexpression in smokers with COPD peripheral blood samples (18), indicating its momentous involvement in COPD. In addition,

lncRNA MEG3 knockdown inhibited CSE-induced apoptosis and inflammation of 16HBE cells, providing a possible therapeutic target for CSE-induced COPD (19). However, the effect of lncRNA MEG3 derived form CSE-stimulated exosomes in COPD process remains elusive.

Through bioinformatics predication, we found multiple methylation sites on TREM-1 mRNA, and there may be bindings between N6-methyladenosine (m^6A) transferase METTL3 and TREM-1 in macrophages. Furthermore, lncRNA MEG3 may bind to spleen focus forming virus proviral integration oncogene (SPI1) protein, and there were binding sites between SPI1 and methyltransferase 3 (METTL3). Existing evidence has revealed the role of RNA methylation of m^6A in COPD (20,21). METTL3, an important m^6A writer, was measured to be elevated in CSE-induced human bronchial epithelial cells (22). Ultimately, we speculated that lncRNA MEG3 might activate METTL3 by recruiting SPI1 and finally upregulate TREM-1. Herein, our research addressed the mechanism of CSE-treated MAECs-derived exosomal lncRNA MEG3 in M1 macrophage polarization and pyroptosis during COPD via SPI1/METTL3/TREM-1, hoping to offer theoretical basis for the development of potential therapeutic targets for COPD.

MATERIALS AND METHODS

Preparation of CSE

As previous description (23), a non-filtered Furong cigarette (carbon monoxide: 14 mg/cigarette; nicotine: 1.0 mg; tar: 13 mg) was burned and the smoke was completely dissolved in 4 mL PBS through a tube as the original CSE (100% concentration). The CSE solution was filtered with a 0.22 μm filter and used within 30 min.

Cell culture and transfection

MAECs (Newgainbio, Wuxi, China) and mouse macrophages (RAW264.7; American Type Culture Collection, Manassas, VA, USA) were cultured in high-glucose- DMEM (Thermo Fisher Scientific, Waltham, MA, USA) containing 10% FBS (ScienCell, Carlsbad, CA, USA), 100 U/ml penicillin, and 100 mg/ml streptomycin under the condition of 37°C and 5% CO_2.

Cell transfection was carried out using Lipofectamine 3000 (Invitrogen, Carlsbad, CA, USA) based on the manufacturer's protocol. To be specific, sh-MEG3-transfected MAECs or untransfected MAECs were treated with CSE, followed by exosome isolation. The exosomes were co-cultured with RAW264.7 cells, which were transfected with oe-TREM-1, oe-METTL3, or untransfected. In addition, RAW264.7 cells were transfected with sh-MEG3 or sh-MEG3 + oe-METTL3 to explore the effect of MEG3 expression change on the expression of METTL3 and TREM-1. RAW264.7 cells were transfected with sh-MEG3 or sh-MEG3 + oe-SPI1 to explore the effect of MEG3 expression change on the binding relationship between SPI1 and METTL3.

Isolation and identification of exosomes

MAECs were cultured in DMEM containing 10% exosome-depleted FBS (Thermo Fisher Scientific), followed by exposure to 5% CSE (PBS exposure serving as control) for 12 h after 70%–80% confluence was reached. Afterward, exosomes were isolated from the medium using ExoQuick-TC PLUS kit (System Biosciences, Mountain View, CA, USA) according to the manufacturer's protocols. The protein concentration of exosomes was quantified using a bicinchoninic acid (BCA) kit (Pierce, Waltham, MA, USA). The morphological characteristics of exosomes were observed under a transmission electron microscope. The size distribution

and concentration of exosomes were analyzed through the nanoparticle tracking analysis system (ZetaView™120, Particle Metrix, Inning am Ammersee, Germany). The expression of exosome markers (CD9 and CD63) and Golgi marker (GM130) was measured by western blotting. The Abs including anti-CD9 (ab223052, 1:2,000, Abcam, Cambridge, UK), anti-CD63 (ab217345, 1:1,000, Abcam), and anti-GM130 (sc-55590, Santa Cruz Biotechnology, Dallas, TX, USA) were employed for exosome identification.

Exosomes were named as follows according to different treatments of MAECs: Exo^{-PBS} (PBS treatment), Exo^{-CSE} (CSE treatment), sh-MEG3-Exo^{-CSE} (sh-MEG3 transfection and CSE treatment), and sh-NC-Exo^{-CSE} (sh-NC transfection and CSE treatment).

Flow cytometry (FCM) analysis

The treated RAW264.7 cells were washed once in pre-cooled PBS and then sealed with 100 μl 0.2% bovine serum albumin in PBS for 45 min. After PBS washing, the RAW264.7 cells were incubated with FITC-labeled anti-CD86 (105005, BioLegend, San Diego, CA, USA) in dark at 4°C for 45 min, followed by the detection of the percentage of CD86-positive (CD86$^+$) cells on FACSCalibur via Cell-Quest software (Becton-Dickinson, San Jose, CA, USA).

Establishment of a COPD mouse model and groups

Forty-eight male C57BL/6J mice (specific pathogen-free, 20–25 g, 6–8 wk) were obtained from Charles River (Beijing, China) and raised under conditions of 25°C±1°C temperature and 55%±5% humidity with a 12-h light/dark cycle. All mice had ad libitum access to food and water. All animal experiments in this study were approved by the Research Ethics Committee of Xiangya Hospital, Central South University (No. 2022020338).

The CS exposure was conducted to simulate COPD *in vivo*. In short, mice were placed in a homemade plexiglass box and directly exposed to unfiltered CS from five Furong cigarettes. CS exposure was performed four times a day (smoke-free interval of 30 min) for 15 wk with continuous six days a week. Mice were randomly grouped into CON (n=6, air exposure), COPD (n=12, CS exposure), COPD + sh-NC-Exo^{-CSE} (n=12, CS exposure), COPD + sh-MEG3-Exo^{-CSE} (n=12, CS exposure), and COPD + sh-MEG3-Exo^{-CSE} + oe-TREM-1 groups (n=6, CS exposure). After CS exposure, mice in the COPD + sh-NC-Exo^{-CSE} and COPD + sh-MEG3-Exo^{-CSE} groups were injected with sh-NC-Exo^{-CSE} and sh-MEG3-Exo^{-CSE} (10 μg of protein concentration was dispersed in 200 μl PBS) via tail vein, respectively, and mice in the COPD + sh-MEG3-Exo^{-CSE} +oe-TREM-1 group underwent tail vein injection of sh-MEG3-Exo^{-CSE} and intranasal instillation of 50 μl oe-TREM-1 lentivirus (4×10^8 PFU/mouse), once every two wk. The lentivirus of oe-TREM-1 or oe-NC was provided by Hanbio Biotechnology (Shanghai, China).

Determination of mouse lung function

Mice underwent anesthesia by pentobarbital (50 mg/kg), and then the mouse's trachea was inserted with a Y-type endotracheal cannula connected with a flow sensor (HX200, Beijing Xinghangxingye Corporation, Beijing, China) to measure the forced expiratory volume in 0.4 s/forced vital capacity (FEV0.4/FVC) and peak expiratory flow (PEF).

Bronchoalveolar lavage (BAL) and lung tissue processing

Subsequent to anesthesia, the chest of mouse was opened for BAL. Aliquots of PBS (800 μl) were infused into the lung of mouse through the tracheal opening and then withdrawn gently. Three times of BAL was conducted with the same syringe. The BAL fluid (BALF) was gathered and centrifuged at 2,000 g for 10 min with the cell-free supernatant stored at −80°C for cytokine

assessment and reverse transcription quantitative PCR (RT-qPCR) analysis. After the removal of the lung tissues of mice, a part of tissues underwent fixation, paraffin embedding, and sectioning (5 μm) for H&E, immunofluorescence, and immunohistochemical staining assays, and the other part of tissues was stored at −80°C for subsequent gene and protein detection.

Immunohistochemical staining

After dewaxing and hydration, sections were incubated with anti-TREM-1 (MA5-16765, Invitrogen), anti-METTL3 (ab195352, Abcam), and anti-SPI1 (#2258, CST, Beverly, MA, USA) overnight (4°C) and then probed with a secondary Ab for 2 h at room temperature. Subsequent to color development with diaminobenzidine, the sections received counterstaining in hematoxylin (35 s), dehydration, and sealing. After drying, the images were captured under a microscope.

H&E staining

Following dewaxing and hydration of sections, H&E staining was performed according to the standard protocols of the kit (Solarbio, Beijing, China). The slides were observed under a light microscope with six visual fields that avoid blood vessels and trachea, followed by photographing for histopathology assessment. Each image was recorded including photo length (L), the number of alveolar space (Ns), the number of alveoli (Na), and photo size (S), with the formula: mean linear intercept (MLI) = L/Ns; mean alveolar number (MAN) = Na/S. MLI reflects the mean alveolar diameter and MAN reflects alveolar density. The severity of emphysema in COPD was evaluated by measuring the difference of MLI and MAN values in lung histommorphology.

Immunofluorescence staining

After dewaxing and hydration, sections were treated with microwave Ag extraction method, and endogenous peroxidase was inactivated with 3% H_2O_2, followed by section sealing with 10% goat serum for 30 min. Thereafter, the sections received overnight incubation (4°C) with anti-CD68 (ab283654, Abcam) and 1-h incubation (room temperature) with Cy3-conjugated secondary Ab (1:1,000, Life Technologies, Gaithersburg, MD, USA). The nucleus was stained by 4',6-diamidino-2-phenylindole (Beyotime, Shanghai, China), followed by observation under a fluorescence microscope and counting of CD68-positive ($CD68^+$) cells. Three visual fields were randomly selected from each section and the average was recorded.

RT-qPCR

Total RNA was extracted from RAW264.7 cells and mouse BALF and lung tissues using TRIzol reagents (Invitrogen), followed by reverse transcription into cDNA with iScript cDNA kit (Bio-Rad, Hercules, CA, USA). RT-qPCR was carried out using SYBR Green PCR mix (Applied Biosystems, Foster City, CA, USA) with GAPDH as the internal reference. The relative expression of target genes was calculated by the $2^{-\Delta\Delta Ct}$ method. Primers are listed in **Table 1**.

Western blotting

Total protein was extracted from exosomes, cultured RAW264.7 cells, and mouse lung tissues using radio-immunoprecipitation assay (RIPA) lysis buffer (Beyotime), followed by protein concentration measurement with a BCA kit. After that, the protein was separated by 10% sodium dodecyl sulfate-polyacrylamide gel electrophoresis and transferred onto a polyvinylidene fluoride membrane. Subsequent to 1-h sealing in 5% skim milk, the membrane received overnight (4°C) probing with anti-TREM-1 (MA5-16765, Invitrogen),

Table 1. Primer sequences used in RT-qPCR analysis

Name of primer	Sequences
lncRNA MEG3-F	AGTGCCTTGTAAATCGCCCG
lncRNA MEG3-R	ACTGCATTTGTCTCCTGCGT
SPI1-F	GTCACCCCAAGGGGACTATC
SPI1-R	GCCGAGAGAGAAAGGTGTCG
METTL3-F	GACTCTGGGCACTTGGGTGAG
METTL3-R	GAAACAGCATCAGTGGGCAAG
TREM-1-F	CTTTGTCTCAGGTTCTTCAGATG
TREM-R	TCCTGTGAAATAGACACCGC
iNOS-F	ATTTCACCTGCAACAGGGAG
iNOS-R	CTCCACTGCCCCAGTTTTTG
GAPDH-F	CCCTTAAGAGGGATGCTGCC
GAPDH-R	TACGGCCAAATCCGTTCACA

F, forward; R, reverse.

anti-GAPDH (ab9485, Abcam), anti-METTL3 (ab195352, Abcam), anti-SPI1 (#2258, CST), anti-NOD-like receptor family pyrin domain containing 3 (NLRP3) (#15101, CST), anti-apoptosis-associated speck-like protein containing a caspase-1 recruitment domain (ASC) (#67824, CST), anti-caspase-1 (#9662, CST), anti-cleaved-caspase-1 (#89332, CST), anti-gasdermin D (GSDMD) (ab209845, Abcam), and anti-GSDMD-N (#10137, CST), followed by 1-h incubation with a secondary Ab at room temperature. Finally, the bands were visualized using the enhanced chemiluminescence kit (Thermo Fisher Scientific).

ELISA

The levels of TNF-α and IL-1β in RAW264.7 cells and mouse BALF and lung tissues were determined by ELISA kits (R&D Systems, Minneapolis, MN, USA) in strict accordance with the instructions.

Methylated RNA immunoprecipitation (MeRIP)-qPCR

m^6A RIP assay was performed with a Magna MeRIP m^6A kit (Millipore, Darmstadt, Germany). Specifically, the anti-m^6A Ab or anti-IgG Ab was added into IP buffer for 1 h to bind to protein A/G magnetic beads. Later, IP buffer with ribonuclease and protease inhibitors was added with the purified mRNA and bead-Ab complexes overnight at 4°C. RNA was eluted by elution buffer and purified by phenol-chloroform, followed by RT-qPCR on IP products.

Photoactivatable ribonucleoside-enhanced crosslinking and immunoprecipitation (PAR-CLIP)

The binding of METTL3 and TREM-1 mRNA was tested by PAR-CLIP assay. In short, cells experienced 14-h incubation with 200 mM 4-thiopyridine (Sigma Aldrich) and then cross-linked with 0.4 J/cm^2 at 365 nm. After lysis, METTL3 Ab was used for IP assay at 4°C, and protein was removed by protease K enzyme. The RNA was extracted for detection of TREM-1 expression by RT-qPCR.

RNA decay assay

Cells were treated with 5 μg/ml actinomycin D, and TREM-1 mRNA level was evaluated with RT-qPCR at 0, 2, 4, 6, and 8 h after the total RNA was obtained with TRIzol reagents.

RIP-qPCR

The Magna RIP kit (EMD Millipore, Billerica, MA, USA) was utilized to conduct RIP assay. Cells (2×10^6 cells/mL) were treated with RIPA buffer after fixation, followed by centrifugation. The collected cell lysis was incubated at 4°C with anti-SPI1 (#2258, CST), anti-METTL3

(ab195352, Abcam), or anti-IgG. Afterward, the cell lysis was added into beads containing protease K, followed by RNA extraction by TRIzol reagents for IP assay. The co-precipitated RNA was purified by RNeasy Mini kits (Qiagen, Hilden, Germany), and the RNA levels were tested by RT-qPCR.

Fractionation of nuclear and cytoplasmic RNA

A nuclear/cytosol fractionation kit (Thermo Fisher Scientific) was used in this assay. The RNA level of lncRNA MEG3 in the cytoplasm and nucleus was assessed by RT-qPCR with GAPDH as a positive control for cytoplasmic RNA and U6 for nuclear RNA.

Chromatin immunoprecipitation (ChIP)-qPCR

An EZ-ChIP™ kit (Millipore, Bedford, MA, USA) was used in ChIP assay. Cells were treated with formaldehyde and then glycine, after which cell precipitation was obtained after centrifugation. The precipitation was suspended in cell lysis containing phenylmethanesulfonyl fluoride solution, followed by centrifugation with the supernatant discarded. After break of DNA by ultrasound in an ice water bath, 90% of lysis was incubated with magnetic beads coupled with anti-SPI1 (#2258, CST) or anti-IgG (10% of supernatant was used as control). Subsequent to centrifugation, the DNA bound to SPI1 protein was eluted, followed by DNA purification with a kit (Beyotime) and quantification of the immunoprecipitated DNA with RT-qPCR.

Dual-luciferase reporter assay

The binding relationship between SPI1 and METTL3 was verified via dual-luciferase reporter assay. The mutant and wild-type sequences of METTL3 with predicted SPI1 binding sites (WT-METTL3 and MUT-METTL3) were cloned into pGL3-Basic reporter vector (Promega Corporation, Madison, WI, USA), followed by co-transfection into RAW264.7 cells with sh-MEG3 or sh-MEG3 + oe-SPI1. Forty-eight h later, the luciferase intensity of each group was evaluated based on the dual-luciferase reporter assay system (Promega Corporation).

Statistical analysis

GraphPad prism 8.0 software was applied for data processing. Data were stated as mean±SD. The *t*-test was applied for comparisons between two groups. The one-way analysis of variance test was adopted for comparisons among multiple groups, with the Tukey's test for post hoc multiple comparisons. The $p<0.05$ meant that the difference was statistically significant.

RESULTS

CSE-treated MAECs-derived exosomal lncRNA MEG3 promotes M1 macrophage polarization and pyroptosis

First, we successfully extracted exosomes from CSE-treated MAECs (**Fig. 1A-C**). Subsequently, we conducted RT-qPCR to test the expression of MEG3 and found high expression of MEG3 in CSE-treated MAECs-derived exosomes (**Fig. 1D**).

To investigate the therapeutic role of exosomal MEG3 in COPD progression via M1 macrophage polarization and pyroptosis, MAECs underwent MEG3 inhibition and CSE treatment before exosome extraction. Results from RT-qPCR revealed that the sh-MEG3-Exo^{-CSE} group had lower expression of MEG3 than the sh-NC-Exo^{-CSE} group (**Fig. 1E**). Thereafter, macrophages were treated with the extracted exosomes for 48 h. Compared with the Exo^{-PBS}

https://doi.org/10.4110/in.2024.24.e3

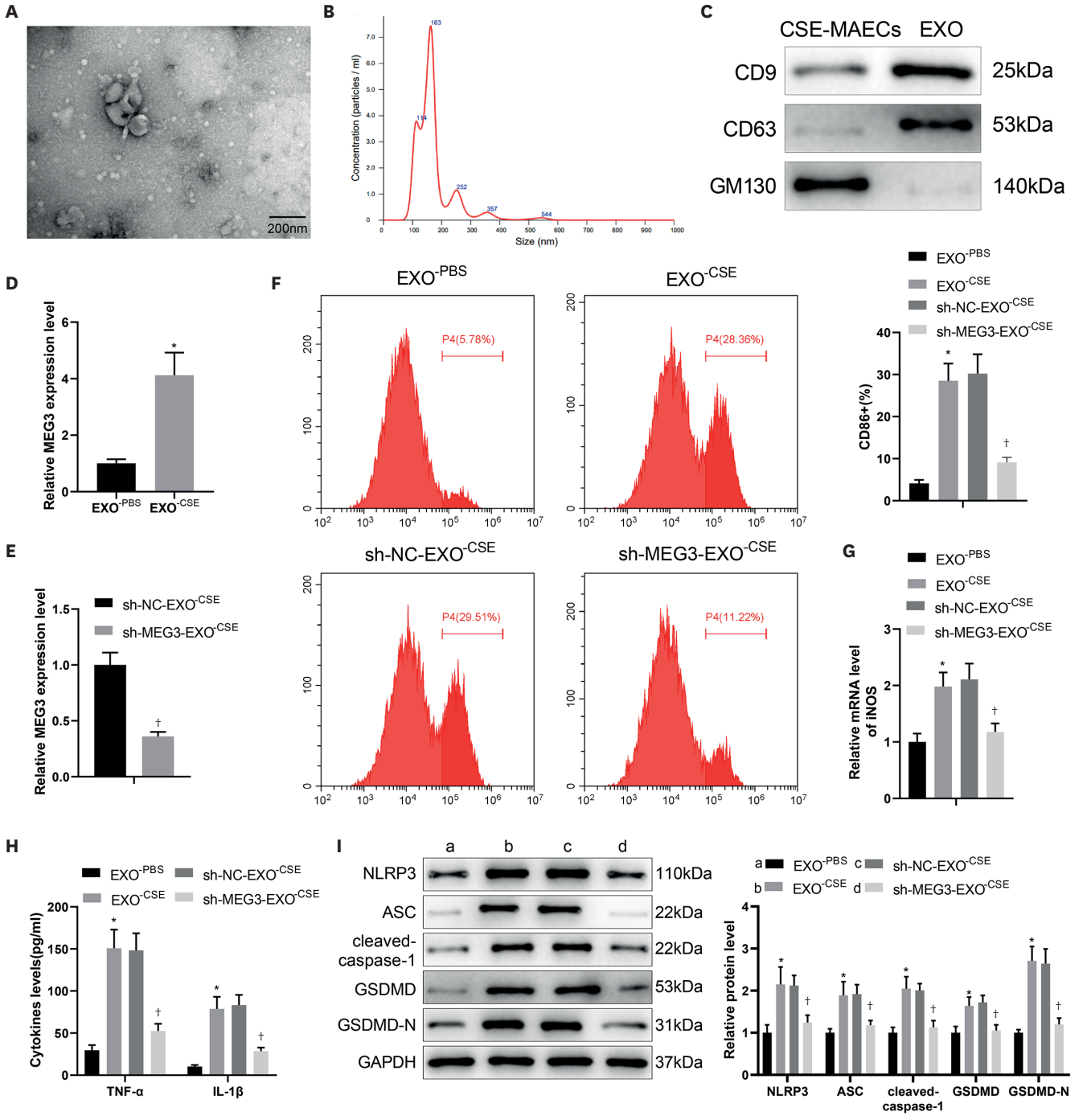

Figure 1. Exosomal lncRNA MEG3 derived from CSE-treated MAECs accelerates M1 macrophage polarization and pyroptosis. (A) The morphology of exosomes was observed by TEM. (B) The particle size of exosomes was measured via nanoparticle tracking analysis system. (C) The expression of exosome markers (CD9 and CD63) and Golgi marker (GM130) was tested through western blotting. (D) The expression of MEG3 in exosomes from CSE-treated MAECs was detected by RT-qPCR. After MAECs underwent MEG3 inhibition and CSE treatment before exosome extraction, (E) the expression of MEG3 in exosomes was tested by RT-qPCR. After macrophages were treated with the extracted exosomes for 48 h, (F) the percentage of $CD86^+$ cells in macrophages was evaluated by FCM analysis. (G) The mRNA level of M1 macrophage marker iNOS was examined by RT-qPCR. (H) The levels of TNF-α and IL-1β in supernatant were assessed by ELISA. (I) The levels of pyroptosis-related proteins (NLRP3, ASC, cleaved-caspase-1, GSDMD, and GSDMD-N) were detected by western blotting (n=3).*$p<0.05$, compared with the Exo^{-PBS} group; †$p<0.05$, compared with the sh-NC-Exo^{-CSE} group.

https://doi.org/10.4110/in.2024.24.e3

group, the Exo^{-CSE} group had an elevated percentage of CD86^{+} cells (**Fig. 1F**), increased iNOS (M1 macrophage marker) mRNA level (**Fig. 1G**), and enhanced TNF-α and IL-1β levels in macrophages (**Fig. 1H**), while these in the sh-MEG3-Exo^{-CSE} group were decreased versus the sh-NC-Exo^{-CSE} group (**Fig. 1F-H**). Western blotting showed that the protein levels of pyroptosis-related proteins NLRP3, ASC, caspase-1, cleaved-caspase-1, GSDMD, and GSDMD-N were elevated in the Exo^{-CSE} group (vs. Exo^{-PBS} group), which were reversed by MEG3 inhibition (**Fig. 1I**, **Supplementary Fig. 1A**). The above data suggested that CSE-treated MAECs-derived exosomal MEG3 could accelerate M1 macrophage polarization and pyroptosis.

CSE-treated MAECs-derived exosomal lncRNA MEG3 exacerbates lung injury, M1 macrophage polarization, and pyroptosis in COPD mice.

Based on the cellular experimental results, we conducted *in vivo* experiments via COPD mouse modeling (CS exposure) and tail vein injection to further explore the effects of exosomal MEG3 on M1 macrophage polarization and pyroptosis. First, RT-qPCR was designed to assess the expression of MEG3 in lung tissues and BALF of normal mice and COPD mice, which reflected that COPD mice had higher expression of MEG3 than normal mice (**Supplementary Fig. 2A and B**). As manifested in **Fig. 2A and B**, the COPD group had lower PEF and FEV0.4/FVC than the CON group, suggested that COPD mice had severe ventilation dysfunction and abnormal diffusion ability. Related to the COPD group, PEF and FEV0.4/FVC were reduced in the COPD + sh-NC-Exo^{-CSE} group, suggesting further aggravation of lung function in COPD mice. However, the COPD + sh-MEG3-Exo^{-CSE} group had increased PEF and FEV0.4/FVC (vs. the COPD + sh-NC-Exo^{-CSE} group), indicated that MEG3 inhibition relieved lung injury of COPD mice.

Next, we designed H&E staining to evaluate the degree of mouse lung injury and observed that CON mice had normal airway and vascular endothelial structure in lung tissues, and COPD mice had severely damaged lung tissues, shown by thickened bronchial walls, infiltration of inflammatory cells around the airway, and disturbed alveolar tissues, while these conditions in the COPD + sh-NC-Exo^{-CSE} group were aggravated. In comparison with the COPD + sh-NC-Exo^{-CSE} group, the lung injury of COPD mice in the COPD + sh-MEG3-Exo^{-CSE} group was reduced (**Fig. 2C**). As illustrated in **Table 2**, the COPD group had higher MLI and lower MAN than the CON group, while further increased MLI and decreased MAN were noted after sh-NC-Exo^{-CSE} administration, which were negated by MEG3 inhibition. Immunofluorescence staining exhibited that the percentage of CD68^{+} cells in mouse lung tissues was increased in the COPD group (vs. the CON group) and further elevated in the COPD + sh-NC-Exo^{-CSE} group (vs. the COPD group), which was reversed by MEG3 inhibition (**Fig. 2D**).

As expected, we found significantly increased levels of iNOS, TNF-α, and IL-1β in mouse lung tissues and BALF in the COPD group versus the CON group, and further increases of these factor levels in the COPD + sh-NC-Exo^{-CSE} group versus the COPD group; however, MEG3 inhibition decreased the levels of these factors (vs. the COPD + sh-NC-Exo^{-CSE} group) (**Fig. 2E and F**). The same trend was observed in the levels of pyroptosis-related proteins (NLRP3, ASC, caspase-1, cleaved-caspase-1, GSDMD, and GSDMD-N) in mouse lung tissues by western blotting (**Fig. 2G**, **Supplementary Fig. 1B**). Taken together, CSE-treated MAECs-derived exosomal MEG3 could promote lung injury, M1 macrophage polarization, and pyroptosis in COPD mice.

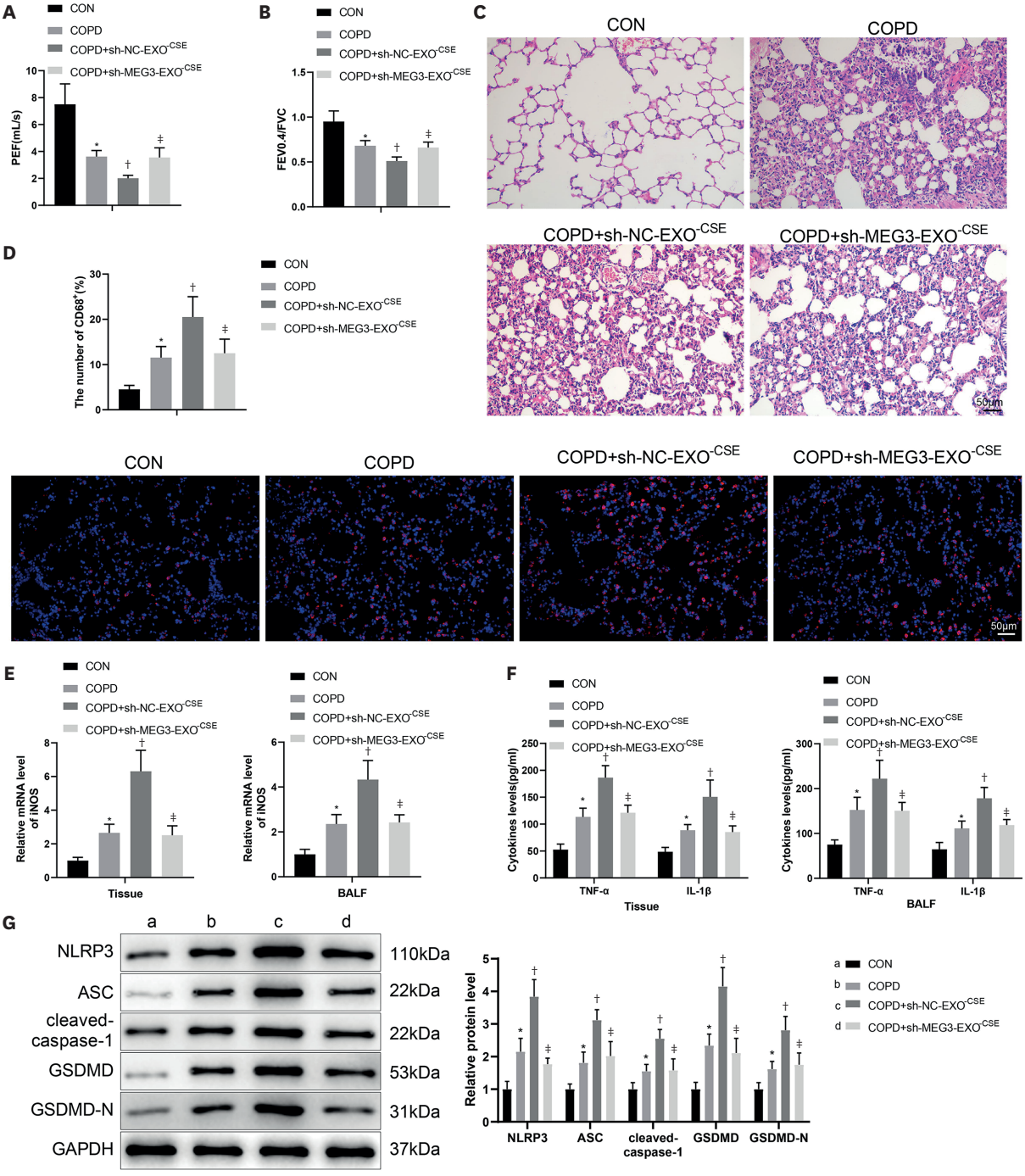

Figure 2. Exosomal lncRNA MEG3 derived from CSE-treated MAECs expedites lung injury, M1 macrophage polarization, and pyroptosis in COPD mice. (A, B) PEF and FEV0.4/FVC were measured to evaluate the lung function of mice. (C) The pathological changes of lung tissue were observed through H&E staining. (D) The percentage of $CD68^+$ cells in mouse lung tissues was detected by immunofluorescence staining. (E) The mRNA level of iNOS in mouse lung tissues and BALF was examined by RT-qPCR. (F) The levels of TNF-α and IL-1β in mouse lung tissues and BALF were assessed by ELISA. (G) The levels of NLRP3, ASC, cleaved-caspase-1, GSDMD, and GSDMD-N in mouse lung tissues were detected by western blotting (n=6).
*$p<0.05$, compared with the CON group; †$p<0.05$, compared with the COPD group; ‡$p<0.05$, compared with the COPD + sh-NC-Exo^{-CSE} group.

https://doi.org/10.4110/in.2024.24.e3

Table 2. Comparisons of MLI and MAN in each group of mice

Groups	MLI (μm)	MAN (number/mm^2)
CON group	51.22±5.12	166.54±23.11
COPD group	88.74±20.13*	91.67±10.15*
COPD + sh-NC-Exo^{-CSE} group	154.25±18.43†	52.03±4.43†
COPD + sh-MEG3-Exo^{-CSE} group	92.13±18.43‡	86.32±11.32‡

*vs. the CON group; †vs. the COPD group; ‡vs. the COPD + sh-NC-Exo^{-CSE} group.

CSE-treated MAECs-derived exosomal lncRNA MEG3 facilitates M1 macrophage polarization and pyroptosis by upregulating TREM-1

Previous evidence illustrated that CSE-treated MAECs-derived exosomes induced M1 macrophage polarization by promoting TREM-1 expression, ultimately expediting COPD progression (12). However, which molecules in exosomes mediate the expression of TREM-1 deserves further study. In this study, we detected an increased TREM-1 expression in the Exo^{-CSE} group (vs. Exo^{-PBS} group), while MEG3 inhibition declined TREM-1 expression (**Fig. 3A**). In COPD mice, we observed an elevated expression of TREM-1 (vs. CON mice) and further elevated TREM-1 following sh-NC-Exo^{-CSE} treatment, which could be negated by MEG3 inhibition (**Fig. 3B**). Based on the above findings, we conjectured that exosomal MEG3 may promote M1 macrophage polarization and pyroptosis by increasing TREM-1 expression.

Subsequently, macrophages were successfully transfected with oe-TREM-1 (**Fig. 3C and D**), followed by co-culture with CSE-treated MAECs-derived exosomes after MEG3 inhibition. The data of FCM, RT-qPCR and ELISA depicted that the percentage of CD86$^+$ cells (**Fig. 3E**) and the levels of iNOS (**Fig. 3F**), TNF-α, and IL-1β (**Fig. 3G**) were reduced in the sh-MEG3-Exo^{-CSE} + oe-NC group versus the sh-NC-Exo^{-CSE} + oe-NC group, whereas opposite results were displayed in the sh-MEG3-Exo^{-CSE} + oe-TREM-1 group (vs. the sh-MEG3-Exo^{-CSE} + oe-NC group). Consistently, western blotting demonstrated that the sh-MEG3-Exo^{-CSE} + oe-NC group had lower levels of NLRP3, ASC, caspase-1, cleaved-caspase-1, GSDMD, and GSDMD-N than the sh-NC-Exo^{-CSE} + oe-NC group, but opposite results of these protein levels were observed in the sh-MEG3-Exo^{-CSE} + oe-TREM-1 group (vs. the sh-MEG3-Exo^{-CSE} + oe-NC group) (**Fig. 3H**, **Supplementary Fig. 1C**). Altogether, CSE-treated MAECs-derived exosomal MEG3 expedited pyroptosis and M1 macrophage polarization by enhancing TREM-1 expression.

METTL3 is highly expressed in COPD mice and macrophages treated with CSE-treated MAECs-derived exosomes

On the basis of the above findings, we delved into the specific mechanisms by which exosomal MEG3 played a role in COPD via TREM-1. At first, we found multiple m^{6}A methylation sites on TREM-1 mRNA through SRAMP (http://www.cuilab.cn/sramp) analysis (**Fig. 4A**), suggested that TREM-1 may be a potential target for m^{6}A methylation modification. Me-RIP was performed to test the TREM-1 m^{6}A level in macrophages and mice. Results in cellular assays displayed that TREM-1 m^{6}A level was significantly increased in the Exo^{-CSE} group (vs. the Exo^{-PBS} group) but decreased in the sh-MEG3-Exo^{-CSE} group (vs. sh-NC-Exo^{-CSE} group) (**Fig. 4B**). Data from animal assays showed that TREM-1 m^{6}A level was markedly elevated in the COPD group versus the CON group, and sh-NC-EXO^{-CSE} treatment further increased TREM-1 m^{6}A level, which was reversed by MEG3 inhibition (**Fig. 4C**).

Thereafter, we used the m^{6}A2target database (http://rm2target.canceromics.org/#/home) to predict the proteins that might bind to TREM-1 mRNA and found that m^{6}A transferase METTL3 might bind to TREM-1 in macrophages, which demonstrated that TREM-1 mRNA may be modulated by METTL3-mediated m^{6}A methylation (**Fig. 4D**). As revealed by RT-qPCR

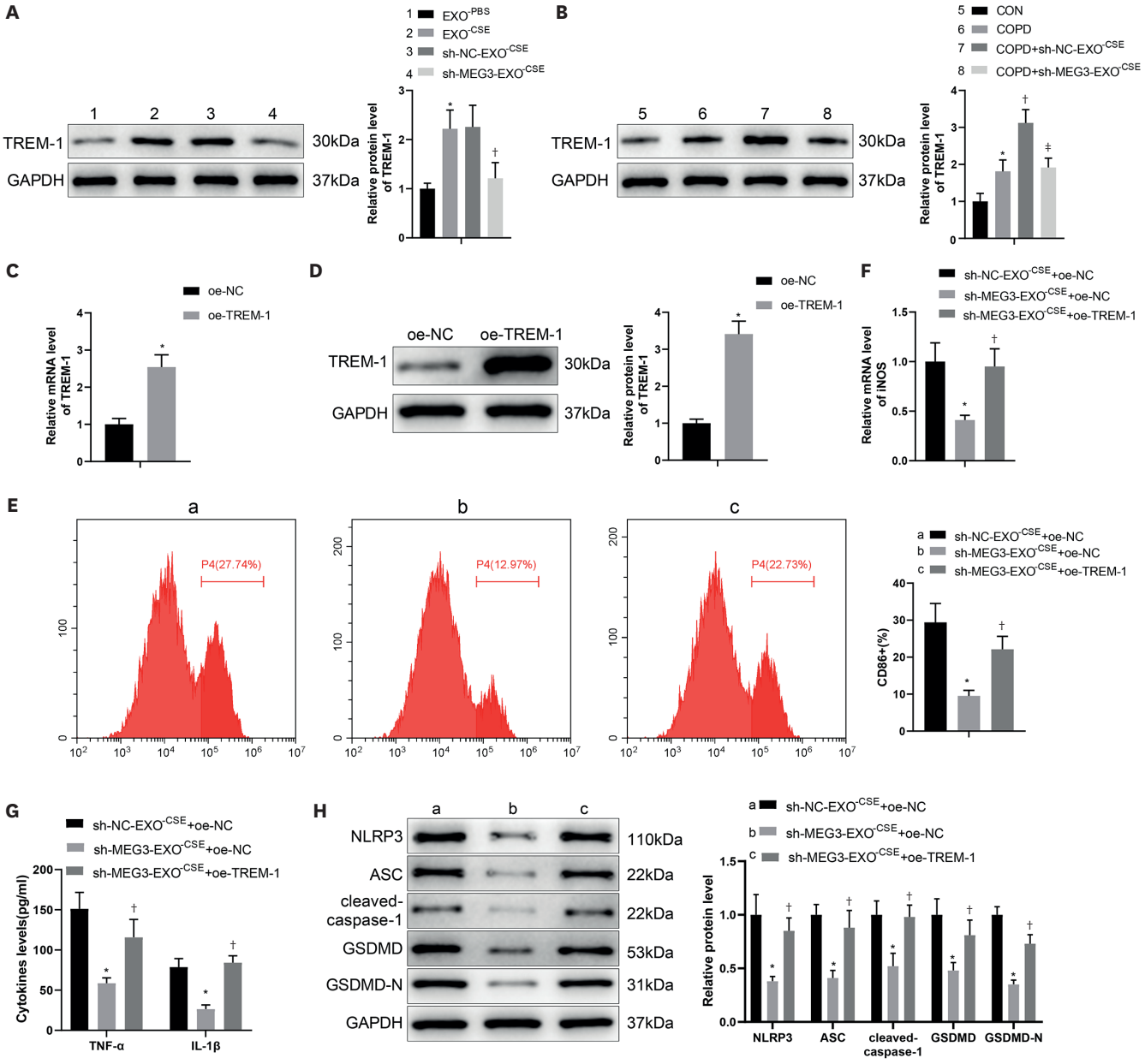

Figure 3. Exosomal lncRNA MEG3 derived from CSE-treated MAECs expedites pyroptosis and M1 macrophage polarization by enhancing TREM-1 expression. (A, B) Western blotting was used to assess the expression of TREM-1 in cells and mice. After macrophages were transfected with oe-TREM-1, (C, D) the transfection efficiency was measured using RT-qPCR and western blotting. After co-culture, (E) the percentage of $CD86^+$ cells was evaluated by FCM analysis. (F) The mRNA level of M1 macrophage marker iNOS was examined by RT-qPCR. (G) The levels of TNF-α and IL-1β in supernatant were assessed by ELISA. (H) The levels of pyroptosis-related proteins (NLRP3, ASC, cleaved-caspase-1, GSDMD, and GSDMD-N) were detected by western blotting (n=3).
*p<0.05, compared with the Exo^{-PBS}, CON, oe-NC, or sh-NC-Exo^{-CSE} + oe-NC group; †p<0.05, compared with the sh-NC-Exo^{-CSE}, COPD, or sh-MEG3-Exo^{-CSE} + oe-NC group; ‡p<0.05, compared with the COPD + sh-NC-Exo^{-CSE} group.

and western blotting, the Exo^{-CSE} group had higher METTL3 expression than the Exo^{-PBS} group, while the sh-MEG3-Exo^{-CSE} group had lower METTL3 expression than the sh-NC-Exo^{-CSE} group (**Fig. 4E and F**). In contrast to the CON group, the expression of METTL3 in mouse lung tissues was greatly augmented in the COPD group, which was further enhanced by sh-NC-EXO^{-CSE} treatment. Conversely, MEG3 inhibition markedly declined METTL3 expression (**Fig. 4G and H**). Collectively, METTL3 expressed at a high level in COPD mice and macrophages treated with CSE-treated MAECs-derived exosomes. MEG3 inhibition

https://doi.org/10.4110/in.2024.24.e3

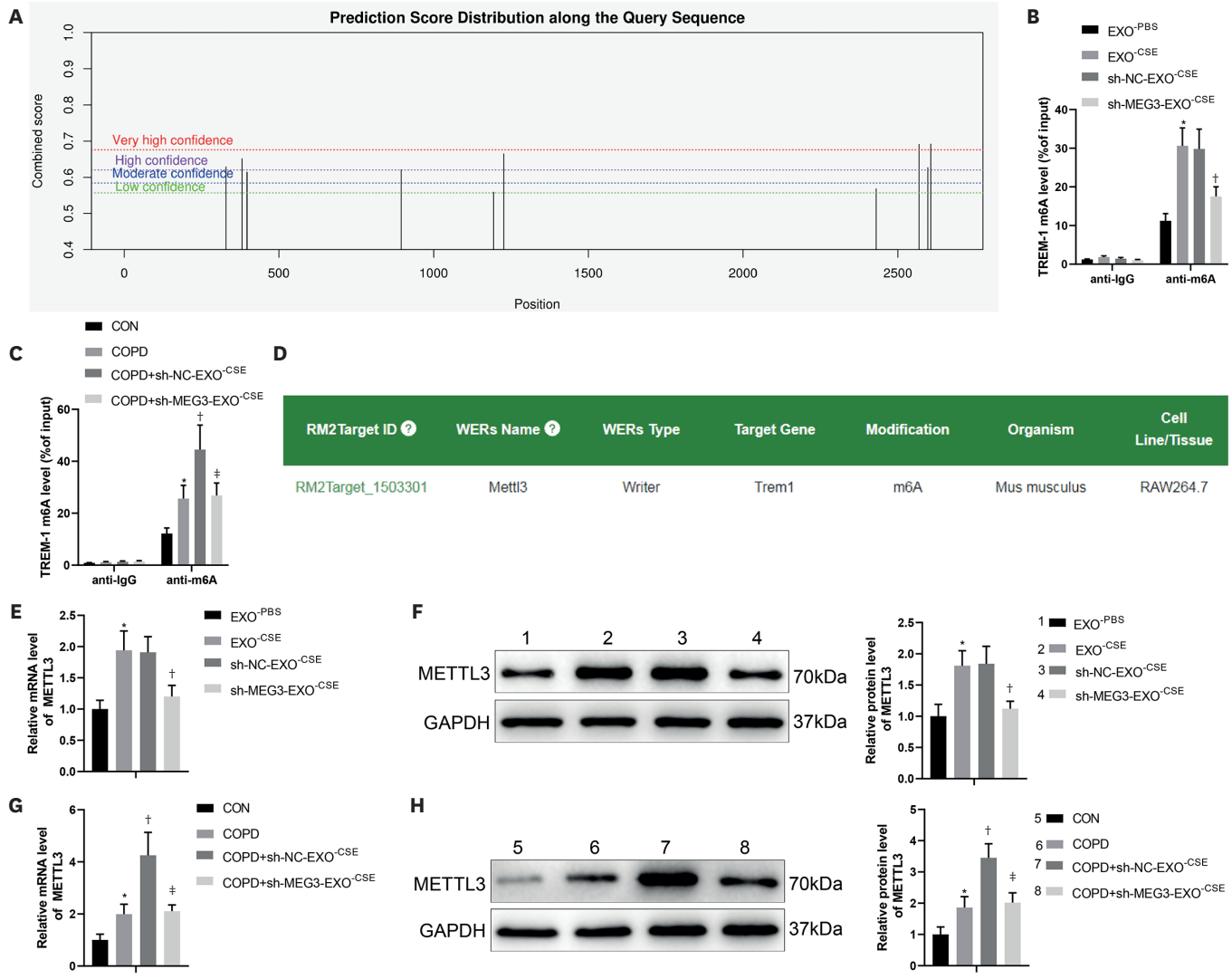

Figure 4. METTL3 expresses at a high level in COPD mice and macrophages treated by CSE-treated MAECs-derived exosomes. (A) The m^{6}A methylation sites on TREM-1 mRNA was analyzed through SRAMP (http://www.cuilab.cn/sramp). (B, C) Me-RIP was conducted to test TREM-1 m^{6}A level in macrophages and mice. (D) m^{6}A2target database (http://rm2target.canceromics.org/#/home) was used to predict the proteins that might bind to TREM-1 mRNA. (E, F) The expression of METTL3 in macrophages was measured by RT-qPCR and western blotting. (G, H) The expression of METTL3 in mouse lung tissues was determined by RT-qPCR and western blotting. Cellular experiments were conducted 3 times; animal experiments (n=6).
*p<0.05, compared with the Exo^{-PBS} or CON group; †p<0.05, compared with the sh-NC-Exo^{-CSE} or COPD group; ‡p<0.05, compared with the COPD + sh-NC-Exo^{-CSE} group.

diminished METTL3 expression in COPD mice and macrophages. These results indicated that MEG3 may promote TREM-1 through METTL3.

LncRNA MEG3 enhances the m^{6}A methylation of TREM-1 via METTL3

To verify whether MEG3 upregulated TREM-1 expression through METTL3-mediated m^{6}A methylation regulation of TREM-1, macrophages were transfected with oe-METTL3 or oe-NC. Results from RT-qPCR and western blotting revealed that METTL3 was successfully overexpressed in macrophages, and an increase of TREM-1 expression was noted in the oe-METTL3 group (vs. the oe-NC group) (**Fig. 5A and B**). Me-RIP reflected that TREM-1 m^{6}A level was markedly stimulated in the oe-METTL3 group (vs. the oe-NC group) (**Fig. 5C**). PAR-CLIP data evinced that with METTL3 as Ab, the pull-down mRNA level of TREM-1 was significantly promoted after METTL3 overexpression (**Fig. 5D**), indicating the binding of METTL3 with

https://doi.org/10.4110/in.2024.24.e3

TREM-1. Furthermore, RNA stability analysis displayed that TREM-1 mRNA was more stable in the oe-METTL3 group than in the oe-NC group (**Fig. 5E**), which suggested that METTL3 mediated the m^{6}A modification of TREM-1 mRNA.

Next, macrophages were transfected with sh-MEG3 and oe-METTL3, and then the expression of MEG3, METTL3, and TREM-1 was assessed by RT-qPCR and western blotting and TREM-1 m^{6}A level by Me-RIP. In comparison with the sh-NC + oe-NC group, the expression of MEG3, METTL3, and TREM-1was substantially reduced in the sh-MEG3 + oe-NC group; however, the sh-MEG3 + oe-METTL3 group had elevated METTL3 and TREM-1 expression and no change in MEG3 expression (vs. the sh-MEG3 + oe-NC group) (**Fig. 5F and G**). As presented in **Fig. 5H**, TREM-1 m^{6}A level was markedly decreased in the sh-MEG3 + oe-NC group (vs. the sh-NC + oe-NC group) but increased in the sh-MEG3 + oe-METTL3 group (vs. the sh-MEG3 + oe-NC group). Altogether, MEG3 promoted TREM-1 expression via METTL3-mediated m^{6}A modification.

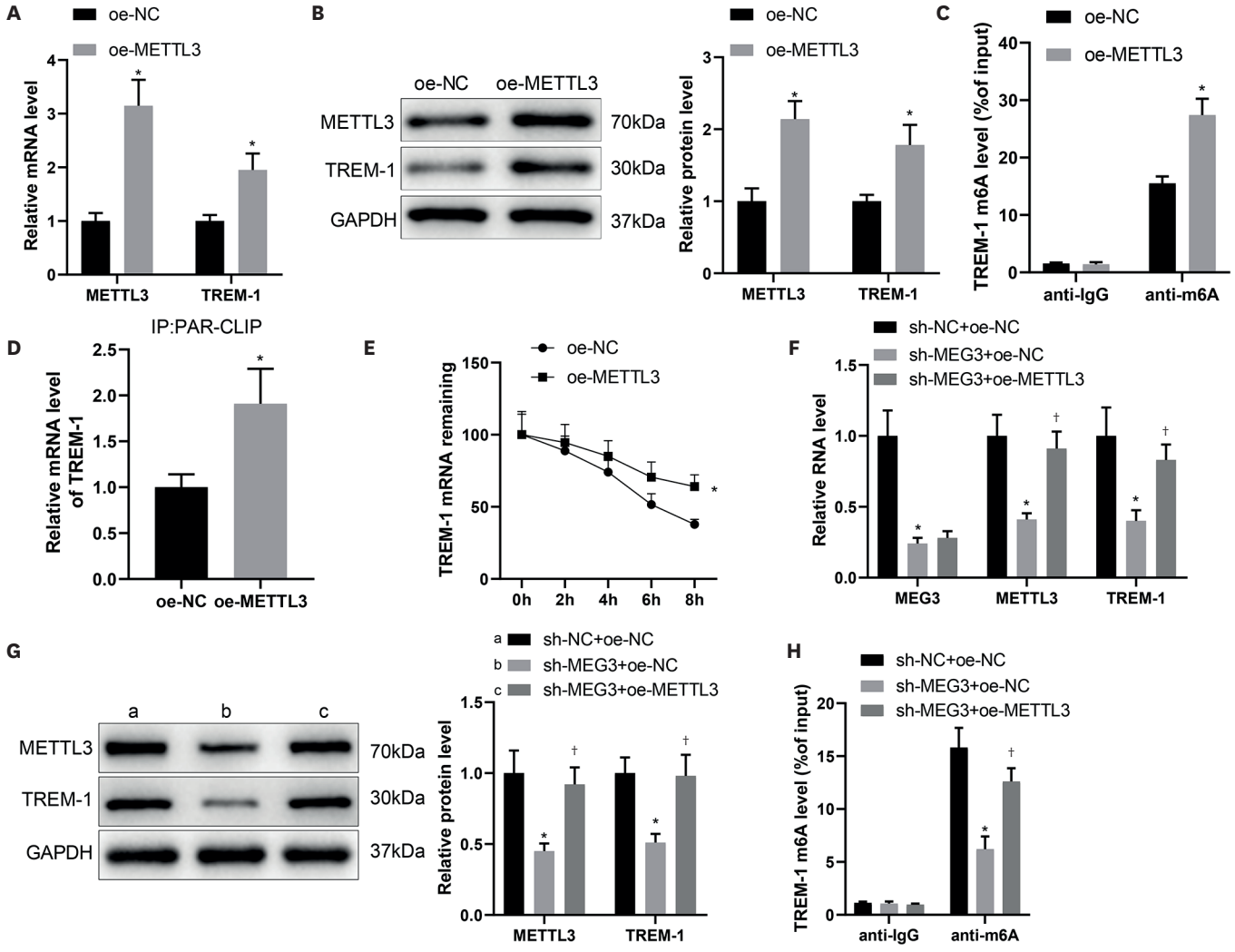

Figure 5. LncRNA MEG3 promotes the m^{6}A methylation of TREM-1 through METTL3. After macrophages were transfected with oe-METTL3, (A, B) the expression of METTL3 and TREM-1 was determined by RT-qPCR and western blotting. (C) TREM-1 m^{6}A level in macrophages was measured by Me-RIP. (D) The binding of METTL3 with TREM-1 mRNA was assessed by PAR-CLIP. (E) RNA stability analysis of TREM-1 after intervention with actinomycin. After macrophages were transfected with sh-MEG3 and oe-METTL3, (F, G) the expression of MEG3, METTL3, and TREM-1 was tested by RT-qPCR and western blotting. (H) TREM-1 m^{6}A level was examined by Me-RIP (n=3).
*p<0.05, compared with the oe-NC or sh-NC + oe-NC group; †p<0.05, compared with the sh-MEG3 + oe-NC group.

https://doi.org/10.4110/in.2024.24.e3

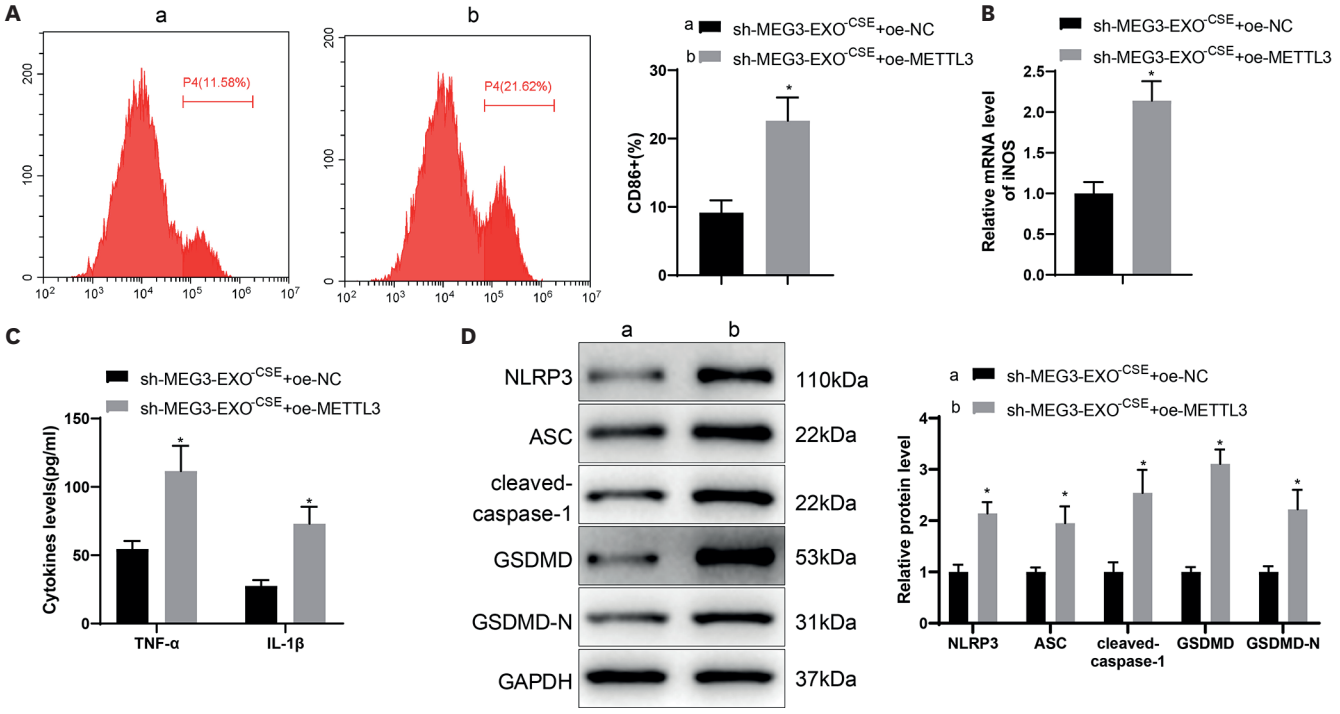

Figure 6. CSE-treated MAECs-derived exosomal lncRNA MEG3 promotes M1 macrophage polarization and pyroptosis by elevating TREM-1 expression via METTL3. After macrophages were transfected with oe-METTL3 and then co-cultured with exosomes derived from CSE-treated and sh-MEG3-transfected MAECs, (A) the percentage of $CD86^+$ cells was evaluated by FCM analysis. (B) The mRNA level of M1 macrophage marker iNOS was examined by RT-qPCR. (C) The levels of TNF-α and IL-1β in supernatant were assessed by ELISA. (D) The levels of pyroptosis-related proteins (NLRP3, ASC, cleaved-caspase-1, GSDMD, and GSDMD-N) were detected by western blotting (n=3).
*$p<0.05$, compared with the sh-MEG3-Exo^{-CSE} + oe-NC group.

CSE-treated MAECs-derived exosomal lncRNA MEG3 expedites M1 macrophage polarization and pyroptosis by upregulating TREM-1 expression via METTL3

Subsequently, macrophages were transfected with oe-METTL3 and then co-cultured with exosomes derived from CSE-treated and sh-MEG3-transfected MAECs. In comparison with the sh-MEG3-Exo^{-CSE} + oe-NC group, the sh-MEG3-Exo^{-CSE} + oe-METTL3 group had increased percentage of $CD86^+$ cells (**Fig. 6A**), iNOS mRNA level (**Fig. 6B**), and TNF-α and IL-1β levels (**Fig. 6C**), accompanied by elevated protein levels of NLRP3, ASC, caspase-1, cleaved-caspase-1, GSDMD, and GSDMD-N (**Fig. 6D**, **Supplementary Fig. 1D**). It was concluded that CSE-treated MAECs-derived exosomal MEG3 promoted M1 macrophage polarization and pyroptosis by elevating TREM-1 expression via METTL3.

LncRNA MEG3 activates METTL3 transcription by recruiting SPI1

Deeply, we verified the relationship between MEG3 and METTL3. RIP-qPCR results unraveled that anti-METTL3 Ab did not significantly enrich MEG3 (**Fig. 7A**), which demonstrated that MEG3 did not regulate TREM-1 through RNA-binding protein mechanism in combination with METTL3. Hence, we speculated that MEG3 might regulate TREM-1 by recruiting transcription factors to activate METTL3. To test this hypothesis, we conducted nuclear/cytosol fractionation of macrophages and then detected the expression of MEG3 using RT-qPCR, which illustrated that MEG3 expression in the nucleus was higher than that in the cytoplasm (**Fig. 7B**). Moreover, RPISeq (http://pridb.gdcb.iastate.edu/RPISeq/) predicted that MEG3 may bind to SPI1 protein (**Fig. 7C**), and Jaspar (https://jaspar.genereg.net/) displayed that there were binding sites between SPI1 and METTL3 (**Fig. 7D**). Results from RT-qPCR

https://doi.org/10.4110/in.2024.24.e3

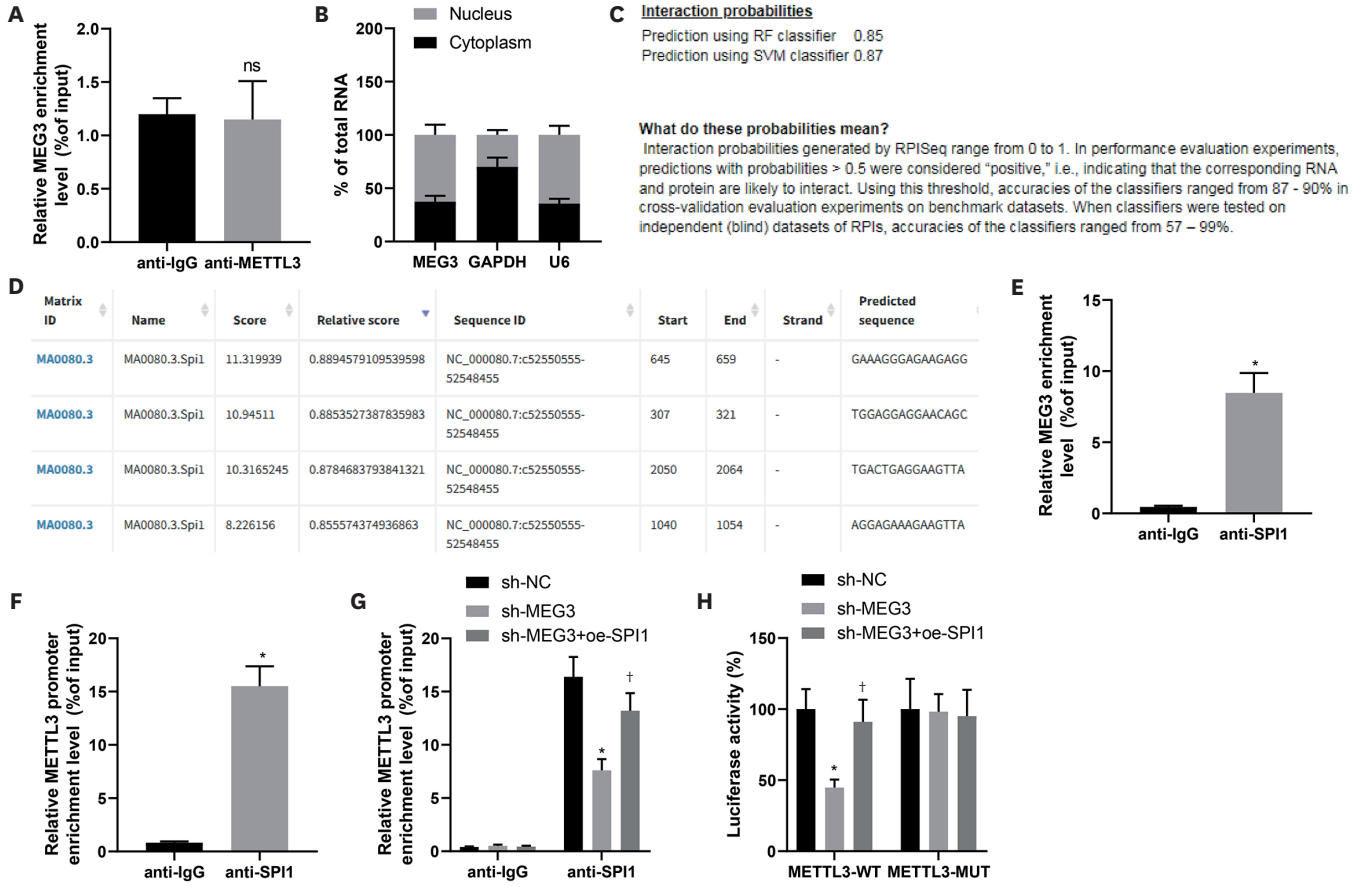

Figure 7. LncRNA MEG3 stimulates METTL3 expression by recruiting SPI1. (A) The binding mechanism between MEG3 and TREM-1 was analyzed via RIP-qPCR. (B) Fractionation of nuclear and cytoplasmic RNA was used to measure the expression of MEG3 in macrophages. (C) RPISeq (http://pridb.gdcb.iastate.edu/RPISeq/) predicted that MEG3 may bind to SPI1 protein. (D) Jaspar (https://jaspar.genereg.net/) displayed that there were binding sites between SPI1 and METTL3. (E) Anti-SPI1 was used in macrophages for RIP-qPCR analysis. (F) Anti-SPI1 was used for ChIP-qPCR analysis. After macrophages were transfected with sh-MEG3 and oe-SPI1, (G) anti-SPI1 was used for ChIP-qPCR analysis. (H) Dual-luciferase reporter assay was used for the binding between SPI1 and METTL3 (n=3). *p<0.05, compared with the anti-IgG or sh-NC group; †p<0.05, compared with the sh-MEG3 group.

unveiled elevated SPI1 mRNA in lung tissues and BALF of COPD mice compared with normal mice (**Supplementary Fig. 2C and D**).

Afterward, we used anti-SPI1 in macrophages for RIP-qPCR and ChIP-qPCR analysis to verify the binding relationship between SPI1 and MEG3 or METTL3. Compared with IgG, MEG3 could be largely enriched with anti-SPI1 Ab (**Fig. 7E**), and the METTL3 promoter enrichment level was increased in the pull-down binding complex of anti-SPI1 Ab (**Fig. 7F**).

To further confirm whether MEG3 promoted METTL3 expression by recruiting SPI1, macrophages were transfected with sh-MEG3 and oe-SPI1. Analysis of ChIP-qPCR showed that MEG3 inhibition weakened the binding between SPI1 and METTL3 promoter, which could be reversed by SPI1 overexpression (**Fig. 7G**). As indicated by dual-luciferase reporter assay (**Fig. 7H**), for METTL3-WT reporter vector, MEG3 inhibition led to a decrease in luciferase activity, which could be partially reversed by SPI1 overexpression; however, MEG3 inhibition and SPI1 overexpression did not affect the luciferase activity of METTL3-MUT vector. In conclusion, MEG3 enhanced TREM-1 expression by recruiting SPI1 to the METTL3 promoter to activate METTL3 expression.

Exosomal lncRNA MEG3 derived from CSE-treated MAECs promotes lung injury, M1 macrophage polarization, and pyroptosis in COPD mice via TREM-1

Finally, we conducted animal experiments to probe the effects of exosomal MEG3-mediated SPI1/METTL3/TREM-1 on COPD mouse lung injury, M1 macrophage polarization, and pyroptosis. Following CS exposure and tail vein injection, mice underwent intranasal instillation with oe-TREM-1 lentivirus. Results from RT-qPCR, western blotting, and immunohistochemical staining reflected that reduced MEG3, METTL3, and TREM-1 expression and no change in SPI1 expression were observed in the COPD + sh-MEG3-Exo^{-CSE} group versus the COPD + sh-NC-Exo^{-CSE} group, while COPD + sh-MEG3-Exo^{-CSE} + oe-TREM-1 group had unchanged expression of MEG3, SPI1, and METTL3 and increased TREM-1 compared with the COPD + sh-MEG3-Exo^{-CSE} group (**Fig. 8A-C**).

Moreover, PEF and FEV0.4/FVC were tested to be higher in the COPD + sh-MEG3-Exo^{-CSE} group than those in the COPD + sh-NC-Exo^{-CSE} group, which were decreased in the COPD + sh-MEG3-Exo^{-CSE} + oe-TREM-1 group versus the COPD + sh-MEG3-Exo^{-CSE} group (**Fig. 8D and E**). From H&E staining results, we noticed thinned bronchial walls, reduced infiltration of inflammatory cells around the airway, and orderly alveolar tissues in mouse lung tissues in the COPD + sh-MEG3-Exo^{-CSE} group (vs. the COPD + sh-NC-Exo^{-CSE} group), whereas oe-TREM-1 instillation aggravated these lung injuries (**Fig. 8F**). Data in **Table 3** reflected that the COPD + sh-MEG3-Exo^{-CSE} group had lower MLI and higher MAN than the COPD + sh-NC-Exo^{-CSE} group, which were abrogated by oe-TREM-1 instillation. Immunofluorescence staining revealed a reduction in CD68^{+} cell number in the COPD + sh-MEG3-Exo^{-CSE} group (vs. the COPD + sh-NC-Exo^{-CSE} group), which was reversed by oe-TREM-1 instillation (**Fig. 9A**).

Additionally, decreased levels of iNOS, TNF-α, and IL-1β in mouse lung tissues and BALF were noted in the COPD + sh-MEG3-Exo^{-CSE} group versus the COPD + sh-NC-Exo^{-CSE} group; however, oe-TREM-1 instillation enhanced the levels of these factors (**Fig. 9B and C**). Consistently, we obtained the same trend in the levels of pyroptosis-related proteins (NLRP3, ASC, caspase-1, cleaved-caspase-1, GSDMD, and GSDMD-N) in mouse lung tissues (**Fig. 9D**, **Supplementary Fig. 1E**).

In summary, CSE-treated MAECs-derived exosomal lncRNA MEG3 aggravated lung injury, M1 macrophage polarization, and pyroptosis in COPD mice via TREM-1.

DISCUSSION

According to the phenotype, macrophages can be polarized into classical activated macrophages (M1) and alternative activated macrophages (M2) under the induction of inflammatory factors and regulation of a variety of information molecules, among which classically activated M1 macrophages play a pro-inflammatory role in COPD progression (24). Furthermore, macrophage pyroptosis is a key node in COPD inflammatory progression (14). Therefore, inhibition of M1 macrophage polarization and pyroptosis benefits COPD management. After a series of experiments *in vitro* and *in vivo*, our work uncovered that MEG3 was highly expressed in CSE-treated MAECs-derived exosomes and may exacerbate lung injury, M1 macrophage polarization, and pyroptosis in COPD mice via the SPI1/METTL3/TREM-1 axis.

Considering that CS is the main risk factor for COPD (25), CS-stimulated mouse models were used for *in vivo* assays in our study. For *in vitro* assays, exosomes were extracted from

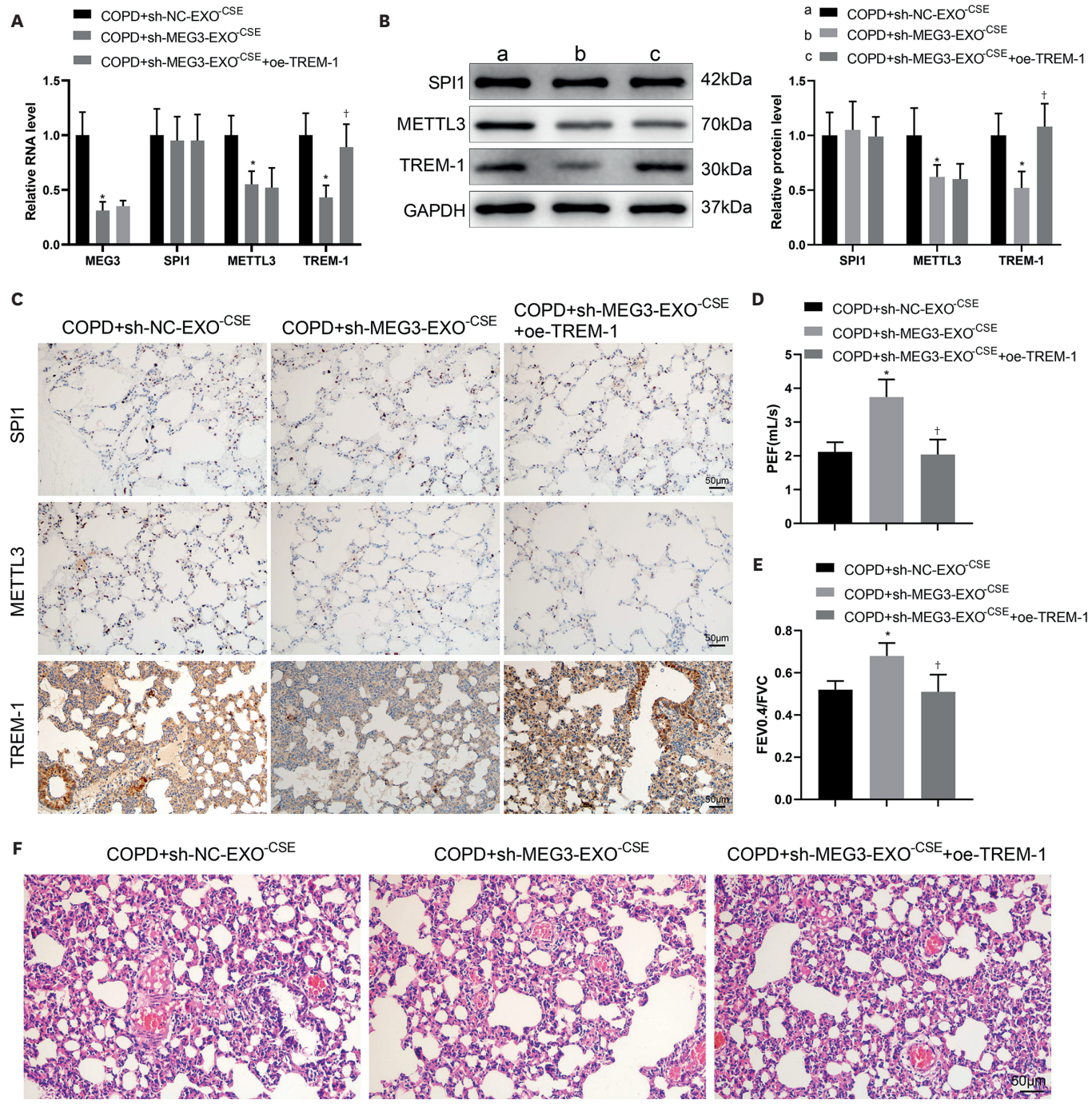

Figure 8. CSE-treated MAECs-derived exosomal lncRNA MEG3 aggravates lung injury in COPD mice via TREM-1. (A) The expression of MEG3, SPI1, METTL3, and TREM-1 was examined by RT-qPCR. (B) the protein expression of MEG3, SPI1, METTL3, and TREM-1 was examined by western blotting. (C) The expression of SPI1, METTL3, and TREM-1 was detected through immunohistochemical staining. (D, E) PEF and FEV0.4/FVC were measured to assess the lung function of mice. (F) The pathological changes of lung tissue were observed through H&E staining (n=6).
*p<0.05, compared with COPD + sh-NC-Exo^{-CSE} group; †p<0.05, compared with the COPD + sh-MEG3-Exo^{-CSE} group.

CSE-treated MAECs, followed by co-culture with macrophages. As our data revealed, CSE-treated MAECs-derived exosomes induced M1 macrophage polarization, pyroptosis, and lung injury in COPD mice, which could be reversed by MEG3 inhibition. Consistently, Chen et al. proved that extracellular vesicles derived from CSE-treated human bronchial epithelial

https://doi.org/10.4110/in.2024.24.e3

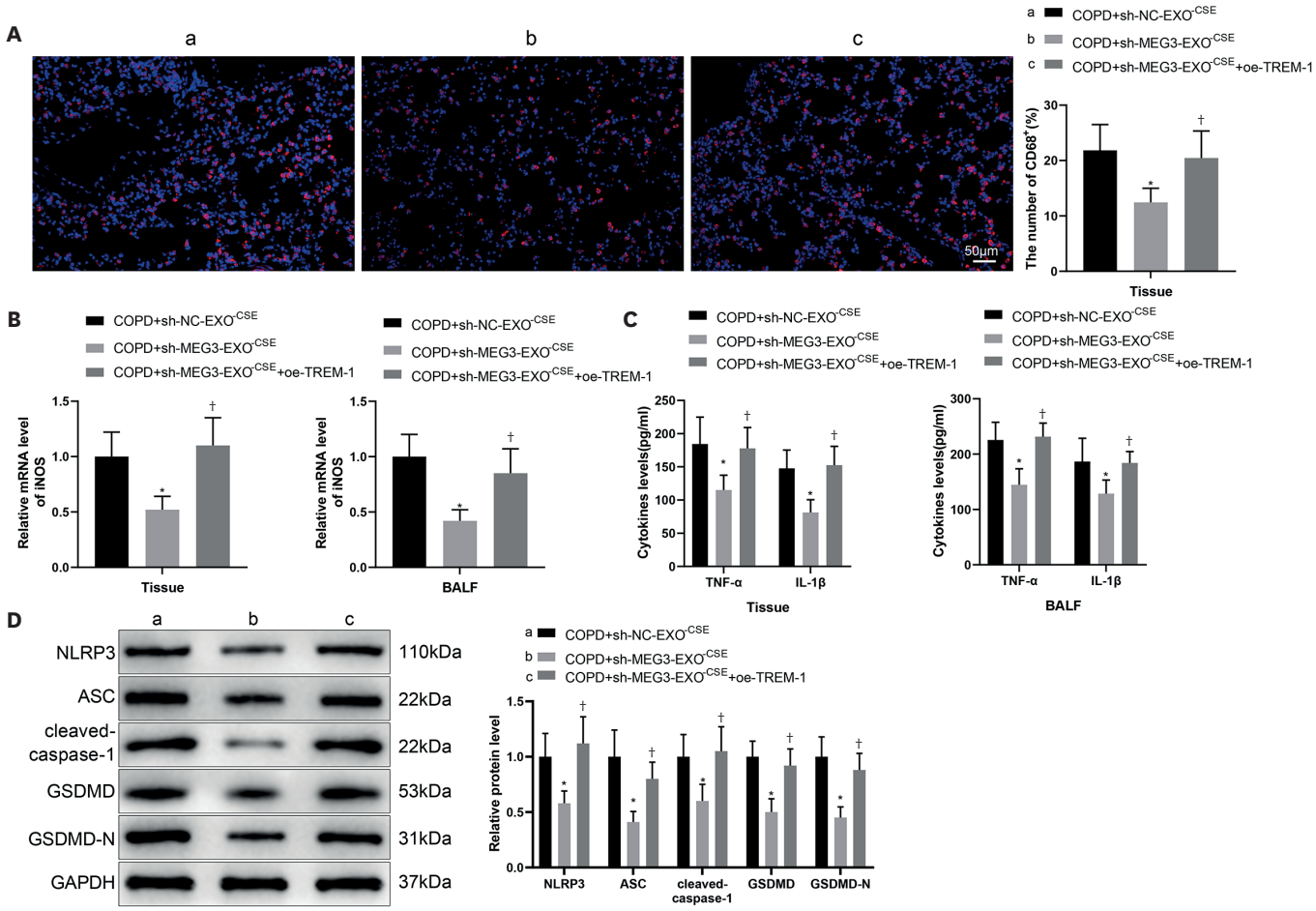

Figure 9. CSE-treated MAECs-derived exosomal lncRNA MEG3 aggravates M1 macrophage polarization, and pyroptosis in COPD mice via TREM-1. (A) The percentage of $CD68^+$ cells in mouse lung tissues was detected by immunofluorescence staining. (B) The mRNA level of iNOS in mouse lung tissues and BALF was examined by RT-qPCR. (C) The levels of TNF-α and IL-1β in mouse lung tissues and BALF were assessed by ELISA. (D) The levels of NLRP3, ASC, cleaved-caspase-1, GSDMD, and GSDMD-N in mouse lung tissues were detected by western blotting (n=6).
*p<0.05, compared with COPD + sh-NC-Exo^{-CSE} group; †p<0.05, compared with the COPD + sh-MEG3-Exo^{-CSE} group.

Table 3. Comparisons of MLI and MAN in each group of mice

Groups	MLI (μm)	MAN (number/mm^2)
COPD + sh-NC-Exo^{-CSE} group	163.21±19.82	48.56±6.24
COPD + sh-MEG3-Exo^{-CSE} group	92.76±22.47*	89.43±10.63*
COPD + sh-MEG3-Exo^{-CSE} + oe-TREM-1 group	152.7±13.84†	52.33±6.04†

*vs. the COPD + sh-NC-Exo^{-CSE} group; †vs. the COPD + sh-MEG3-Exo^{-CSE} group.

cell line could promote M1 macrophage polarization (26). Apparently upregulated MEG3 was observed in human pulmonary microvascular endothelial cells treated with CSE (27) and also in lung tissues of COPD patients (28), which was in accordance with our findings that MEG3 was upregulated in CSE-treated MAECs-derived exosomes. As shown in a subsistent study, MEG3 may trigger inflammatory responses and injury by augmenting the concentration of inflammatory cytokines in multiple major organs, such as liver, heart, and lung (29). Additionally, silencing of MEG3 relieved hyperoxia-induced lung injury by repressing thioredoxin-interacting protein-mediated pyroptosis (30). However, there were no studies about MEG3 released form CSE-derived exosomes in COPD development.

https://doi.org/10.4110/in.2024.24.e3

Next, we focused on the downstream mechanism of MEG3 in COPD. Prior researchers pointed out the elevated TREM-1 expression in COPD patients versus the normal (31), which was consistent with our results that TREM-1 was upregulated in CES-derived exosomes-treated macrophages and COPD mouse lung tissues, which could be reduced by MEG3 inhibition. Further experiments confirmed that overexpressed TREM-1 reversed the mitigative effects of MEG3 inhibition on pyroptosis and M1 macrophage polarization, reflected by increased $CD86^+$ cells and iNOS, TNF-α, IL-1β, NLRP3, ASC, cleaved-caspase-1, GSDMD, and GSDMD-N levels. Similarly, a previous finding revealed that TREM-1 facilitated NLRP3 inflammasome-mediated microglial pyroptosis by elevating the expression of NLRP3, caspase-1, GSDMD, and GSDMD-N, resulting in aggravated neuroinflammation (32). A recent study by Zhong et al indicated that TREM-1 activation caused necroptosis of macrophages, thereby fueling inflammation and aggravating acute lung injury (33). More importantly, compelling evidence suggested that exosomes secreted by CSE-treated MAECs induced M1 macrophage polarization and aggravated CS-induced damage in lung function by enhancing TREM-1 expression (12). Our results were consistent with that of previous studies demonstrating that CSE-treated MAECs-derived exosomal MEG3 expedited pyroptosis and M1 macrophage polarization by elevating TREM-1 expression.

Notably, our data unveiled that TREM-1 mRNA had multiple m^6A methylation sites and regulated by METTL3-mediated m^6A modification. A prior study documented that exposure of cells to CSE increased mRNA expression of METTL3 (34). Reportedly, METTL3 drove M1 macrophage polarization by methylating STAT1 mRNA (35). A study about atherosclerosis has also found that inhibition of hsa_circ_0029589 could promote METTL3 expression, thereby facilitating the inflammation caused by macrophage pyroptosis (36). These observations highlighted the promising function of METTL3 in inflammation. In agreement with previous findings, our work uncovered that METTL3 was increased in COPD mouse lung tissues and CES-treated macrophages, which could be reduced by MEG3 inhibition. Subsequent experiments displayed that overexpression of METTL3 negated the alleviative effects of MEG3 inhibition on M1 polarization and pyroptosis. Overall, MEG3 promoted M1 macrophage polarization and pyroptosis by upregulating the m^6A methylation of TREM-1 via METTL3. Moreover, we found a protein could directly bind to MEG3, namely SPI1. Previously, SPI1 was identified as a candidate target for COPD (37), and increased SPI1 was found in experimental asthma-COPD overlap mouse model (38). Mechanistically, MEG3 elevated TREM-1 expression by recruiting SPI1 to the METTL3 promoter to activate METTL3 expression. Finally, our *in vivo* experiments showed that MEG3 aggravated lung injury, M1 macrophage polarization, and pyroptosis in COPD mice via TREM-1.

In conclusion, our study revealed that lncRNA MEG3 derived from CSE-treated MAECs-derived exosomes may control M1 macrophage polarization and pyroptosis in COPD via the SPI1/METTL3/TREM-1 axis. These findings offered scientific basis for finding novel and efficient therapeutic targets for COPD. According to the reduction principle in the "3Rs" principle based on experimental animals, we have reduced the number of animals used in the experiment as much as possible. Due to the limited cellular and animal sample size, more experiments are needed to support the findings before they can be applied to practical clinical applications. Moreover, in addition to lncRNA MEG3-related mechanisms studied in this work, there may also be other regulatory mechanisms, such as other microRNAs, associated with MEG3 contribution to COPD in inflammation and alveolar remodeling need to be discussed in the future.

ACKNOWLEDGEMENTS

This work was supported by Hunan Provincial Natural Science Foundation of China (Grant No. 2023JJ30943).

SUPPLEMENTARY MATERIALS

Supplementary Figure 1

Detection of caspase-1 expression. Western blotting was used to assess the protein expression of caspase-1 in mouse lung tissues or cells in each group.

Supplementary Figure 2

Detections of lncRNA MEG3 and SPI1 expression. (A, B) The expression of lncRNA MEG3 in lung tissues and BALF of normal mice and COPD mice was detected using RT-qPCR. (C, D) The mRNA expression of SPI1 in lung tissues and BALF of normal mice and COPD mice was detected using RT-qPCR.

REFERENCES

1. Guo P, Li R, Piao TH, Wang CL, Wu XL, Cai HY. Pathological mechanism and targeted drugs of COPD. *Int J Chron Obstruct Pulmon Dis* 2022;17:1565-1575. PUBMED | CROSSREF
2. Vogelmeier CF, Román-Rodríguez M, Singh D, Han MK, Rodríguez-Roisin R, Ferguson GT. Goals of COPD treatment: focus on symptoms and exacerbations. *Respir Med* 2020;166:105938. PUBMED | CROSSREF
3. Alter P, Baker JR, Dauletbaev N, Donnelly LE, Pistenmaa C, Schmeck B, Washko G, Vogelmeier CF. Update in chronic obstructive pulmonary disease 2019. *Am J Respir Crit Care Med* 2020;202:348-355. PUBMED | CROSSREF
4. Brandsma CA, Van den Berge M, Hackett TL, Brusselle G, Timens W. Recent advances in chronic obstructive pulmonary disease pathogenesis: from disease mechanisms to precision medicine. *J Pathol* 2020;250:624-635. PUBMED | CROSSREF
5. Lee KH, Woo J, Kim JY, Lee CH, Yoo CG. Cigarette smoke extract-induced downregulation of p300 is responsible for the impaired inflammatory cytokine response of macrophages. *Cell Signal* 2021;85:110050. PUBMED | CROSSREF
6. Le Y, Wang Y, Zhou L, Xiong J, Tian J, Yang X, Gai X, Sun Y. Cigarette smoke-induced HMGB1 translocation and release contribute to migration and NF-κB activation through inducing autophagy in lung macrophages. *J Cell Mol Med* 2020;24:1319-1331. PUBMED | CROSSREF
7. Wang Y, Smith W, Hao D, He B, Kong L. M1 and M2 macrophage polarization and potentially therapeutic naturally occurring compounds. *Int Immunopharmacol* 2019;70:459-466. PUBMED | CROSSREF
8. Sun J, Li Y. Pyroptosis and respiratory diseases: a review of current knowledge. *Front Immunol* 2022;13:920464. PUBMED | CROSSREF
9. Lee JW, Chun W, Lee HJ, Min JH, Kim SM, Seo JY, Ahn KS, Oh SR. The role of macrophages in the development of acute and chronic inflammatory lung diseases. *Cells* 2021;10:897. PUBMED | CROSSREF
10. Zhang C, Kan X, Zhang B, Ni H, Shao J. The role of triggering receptor expressed on myeloid cells-1 (TREM-1) in central nervous system diseases. *Mol Brain* 2022;15:84. PUBMED | CROSSREF
11. Wang L, Chen Q, Yu Q, Xiao J, Zhao H. TREM-1 aggravates chronic obstructive pulmonary disease development via activation NLRP3 inflammasome-mediated pyroptosis. *Inflamm Res* 2021;70:971-980. PUBMED | CROSSREF
12. Wang L, Chen Q, Yu Q, Xiao J, Zhao H. Cigarette smoke extract-treated airway epithelial cells-derived exosomes promote M1 macrophage polarization in chronic obstructive pulmonary disease. *Int Immunopharmacol* 2021;96:107700. PUBMED | CROSSREF
13. Pegtel DM, Gould SJ. Exosomes. *Annu Rev Biochem* 2019;88:487-514. PUBMED | CROSSREF

14. Zhu Z, Lian X, Su X, Wu W, Zeng Y, Chen X. Exosomes derived from adipose-derived stem cells alleviate cigarette smoke-induced lung inflammation and injury by inhibiting alveolar macrophages pyroptosis. *Respir Res* 2022;23:5. PUBMED | CROSSREF
15. Liu C, Lu J, Yuan T, Xie L, Zhang L. EPC-exosomal miR-26a-5p improves airway remodeling in COPD by inhibiting ferroptosis of bronchial epithelial cells via PTGS2/PGE2 signaling pathway. *Sci Rep* 2023;13:6126. PUBMED | CROSSREF
16. Ouyang C, Wang W, Wu D, Wang W, Ye X, Yang Q. Analysis of serum exosome microRNAs in the rat model of chronic obstructive pulmonary disease. *Am J Transl Res* 2023;15:138-150. PUBMED
17. Han H, Hao L. Revealing lncRNA biomarkers related to chronic obstructive pulmonary disease based on bioinformatics. *Int J Chron Obstruct Pulmon Dis* 2022;17:2487-2515. PUBMED | CROSSREF
18. Lei Z, Guo H, Zou S, Jiang J, Kui Y, Song J. Long non-coding RNA maternally expressed gene regulates cigarette smoke extract induced lung inflammation and human bronchial epithelial apoptosis via miR-149-3p. *Exp Ther Med* 2021;21:60. PUBMED | CROSSREF
19. Fan S, Ren Y, Zhang W, Zhang H, Wang C. Long non-coding maternally expressed gene 3 regulates cigarette smoke extract-induced apoptosis, inflammation and cytotoxicity by sponging miR-181a-2-3p in 16HBE cells. *Oncol Lett* 2021;21:45. PUBMED | CROSSREF
20. Huang X, Lv D, Yang X, Li M, Zhang H. m6A RNA methylation regulators could contribute to the occurrence of chronic obstructive pulmonary disease. *J Cell Mol Med* 2020;24:12706-12715. PUBMED | CROSSREF
21. Hu T, Xu L, Jiang M, Zhang F, Li Q, Li Z, Wu C, Ding J, Li F, Wang J. N6-methyladenosine-methylomic landscape of lung tissues of mice with chronic obstructive pulmonary disease. *Front Immunol* 2023;14:1137195. PUBMED | CROSSREF
22. Zhang Y, Wang L, Liu Y, Yan F. Mettl3-mediated transcriptome-wide m6A methylation induced by cigarette smoking in human bronchial epithelial cells. *Toxicol In Vitro* 2023;89:105584. PUBMED | CROSSREF
23. He S, Chen D, Hu M, Zhang L, Liu C, Traini D, Grau GE, Zeng Z, Lu J, Zhou G, et al. Bronchial epithelial cell extracellular vesicles ameliorate epithelial-mesenchymal transition in COPD pathogenesis by alleviating M2 macrophage polarization. *Nanomedicine* 2019;18:259-271. PUBMED | CROSSREF
24. Li N, Liu Y, Cai J. LncRNA MIR155HG regulates M1/M2 macrophage polarization in chronic obstructive pulmonary disease. *Biomed Pharmacother* 2019;117:109015. PUBMED | CROSSREF
25. Cardoso AOP, Pecli E Silva C, Dos Anjos FF, Quesnot N, Valenca HDM, Cattani-Cavalieri I, Brito-Gitirana L, Valenca SS, Lanzetti M. Diallyl disulfide prevents cigarette smoke-induced emphysema in mice. *Pulm Pharmacol Ther* 2021;69:102053. PUBMED | CROSSREF
26. Chen Z, Wu H, Fan W, Zhang J, Yao Y, Su W, Wang Y, Li P. Naringenin suppresses BEAS-2B-derived extracellular vesicular cargoes disorder caused by cigarette smoke extract thereby inhibiting M1 macrophage polarization. *Front Immunol* 2022;13:930476. PUBMED | CROSSREF
27. Bi H, Wang G, Li Z, Zhou L, Zhang M, Ye J, Wang Z. Long noncoding RNA (lncRNA) maternally expressed gene 3 (MEG3) participates in chronic obstructive pulmonary disease through regulating human pulmonary microvascular endothelial cell apoptosis. *Med Sci Monit* 2020;26:e920793. PUBMED
28. Tang W, Shen Z, Guo J, Sun S. Screening of long non-coding RNA and TUG1 inhibits proliferation with TGF-β induction in patients with COPD. *Int J Chron Obstruct Pulmon Dis* 2016;11:2951-2964. PUBMED | CROSSREF
29. Wu X, Chen D, Yu L. The value of circulating long non-coding RNA maternally expressed gene 3 as a predictor of higher acute respiratory distress syndrome risk and 28-day mortality in sepsis patients. *J Clin Lab Anal* 2020;34:e23488. PUBMED | CROSSREF
30. Zou DM, Zhou SM, Li LH, Zhou JL, Tang ZM, Wang SH. Knockdown of long noncoding RNAs of maternally expressed 3 alleviates hyperoxia-induced lung injury via inhibiting thioredoxin-interacting protein-mediated pyroptosis by binding to miR-18a. *Am J Pathol* 2020;190:994-1005. PUBMED | CROSSREF
31. Wang L, Zhao H, Raman I, Yan M, Chen Q, Li QZ. Peripheral blood mononuclear cell gene expression in chronic obstructive pulmonary disease: miRNA and mRNA regulation. *J Inflamm Res* 2022;15:2167-2180. PUBMED | CROSSREF
32. Xu P, Zhang X, Liu Q, Xie Y, Shi X, Chen J, Li Y, Guo H, Sun R, Hong Y, et al. Microglial TREM-1 receptor mediates neuroinflammatory injury via interaction with SYK in experimental ischemic stroke. *Cell Death Dis* 2019;10:555. PUBMED | CROSSREF
33. Zhong WJ, Zhang J, Duan JX, Zhang CY, Ma SC, Li YS, Yang NS, Yang HH, Xiong JB, Guan CX, et al. TREM-1 triggers necroptosis of macrophages through mTOR-dependent mitochondrial fission during acute lung injury. *J Transl Med* 2023;21:179. PUBMED | CROSSREF
34. Cheng C, Wu Y, Xiao T, Xue J, Sun J, Xia H, Ma H, Lu L, Li J, Shi A, et al. METTL3-mediated m^{6}A modification of ZBTB4 mRNA is involved in the smoking-induced EMT in cancer of the lung. *Mol Ther Nucleic Acids* 2020;23:487-500. PUBMED | CROSSREF

35. Liu Y, Liu Z, Tang H, Shen Y, Gong Z, Xie N, Zhang X, Wang W, Kong W, Zhou Y, et al. The N^6-methyladenosine (m^6A)-forming enzyme METTL3 facilitates M1 macrophage polarization through the methylation of *STAT1* mRNA. *Am J Physiol Cell Physiol* 2019;317:C762-C775. PUBMED | CROSSREF
36. Guo M, Yan R, Ji Q, Yao H, Sun M, Duan L, Xue Z, Jia Y. IFN regulatory factor-1 induced macrophage pyroptosis by modulating m6A modification of circ_0029589 in patients with acute coronary syndrome. *Int Immunopharmacol* 2020;86:106800. PUBMED | CROSSREF
37. Maghsoudloo M, Azimzadeh Jamalkandi S, Najafi A, Masoudi-Nejad A. Identification of biomarkers in common chronic lung diseases by co-expression networks and drug-target interactions analysis. *Mol Med* 2020;26:9. PUBMED | CROSSREF
38. Tu X, Kim RY, Brown AC, de Jong E, Jones-Freeman B, Ali MK, Gomez HM, Budden KF, Starkey MR, Cameron GJM, et al. Airway and parenchymal transcriptomics in a novel model of asthma and COPD overlap. *J Allergy Clin Immunol* 2022;150:817-829.e6. PUBMED | CROSSREF